Proceedings of the Seventh International Conference on
Railway Technology: Research, Development and Maintenance
Edited by: J. Pombo
Civil-Comp Conferences, Volume 15, Paper 10.14
Civil-Comp Press, Edinburgh, United Kingdom, 2026
ISSN: 2753-3239, doi: 10.4203/ccc.15.10.14

Simplified Modelling and Static Validation of Railway Cantilever Structures

S. Sajir, S. Barrans, K. Sztrauch and P. Antunes

Institute of Railway Research, University of Huddersfield, United Kingdom

Abstract

Railway cantilevers support the over-head line (OHL) and are essential to maintain the geometry of contact and messenger wires. Despite their mechanical importance, the cantilever structure is routinely excluded from pantograph-catenary dynamic simulations. In other cases, the support region may be represented through simple boundary conditions, lumped parameters or as a spring-damper. Integrating a detailed cantilever in those pantograph-catenary simulations is impractical and cost sensitive for repeated dynamic analysis.

This paper evaluates whether simplified FEA models can represent the global quasi-static behaviour of Bonomi and single-insulator (SIC) cantilevers in both push-off and pull-off configurations. They were modelled in Abaqus using beam elements and validated with quasi-static experimental testing data under operational static loading derived from BS EN 50119, NR/L2/CIV/073 and NR/L2/CIV/072. Stiffness values were extracted from force-displacement data using linear regression, ranging from 49.90 N/mm to 900.9 N/mm across configurations. The SIC horizontal response was represented most successfully. The SIC vertical response and the Bonomi cases showed where connection flexibility and single-axis displacement measurement limit the simplified model. The results show that a single generic cantilever stiffness is inadequate. It also suggests a need for configuration-specific solutions to represent accurate cantilever behaviour through simplified FEA models.

Keywords: railway overhead line, railway cantilevers, finite element analysis, quasi-static testing, experimental validation, stiffness extraction, pantograph-catenary interaction.

1 Introduction

1.1 Introduction to OHL and railway cantilever

Railway overhead lines transfer electrical power to trains by maintaining controlled contact between the pantograph and the contact wire. The contact wire is supported and positioned through a system of messenger wires, droppers, registration arms, steady arms and mast-mounted cantilever assemblies. The cantilever is the local structural support that connects the wire system to the mast and helps control the wire position at each support location. Figure 1 gives the practical context of the study. It shows the pantograph collecting current from the contact wire, the lateral stagger used to distribute wear across the pantograph head, and the cantilever support assembly that positions the contact and messenger wires at a mast location [1,2,3].

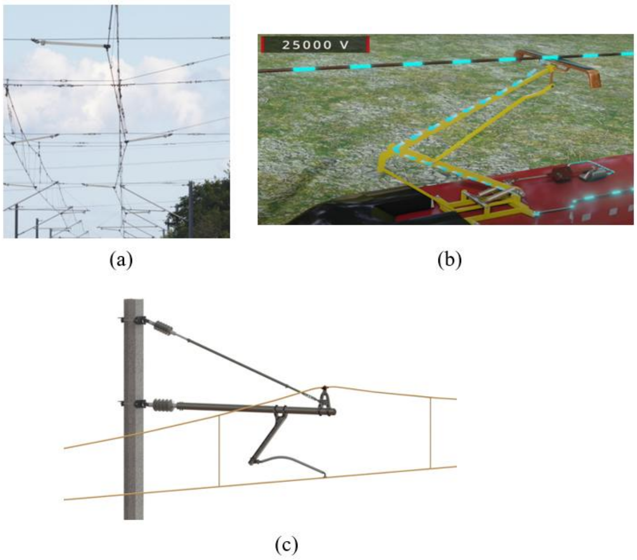

Figure 1: Practical context of the overhead line cantilever, showing (a) contact wire stagger, (b) current collection, and (c) the cantilever support assembly [1,2,3].

Other than being a load-transferring member, the cantilever also forms part of the support boundary condition. It directly influences the contact wire height, lateral stagger and nominal wire position. So, it has an effect on current collection quality and overall pantograph-catenary interaction. For that reason, the cantilever must be assessed under serviceability loading rather than only as a strength component. The serviceability framework used in this paper follows BS EN 50119, NR/L2/CIV/073 and NR/L2/CIV/072 [4,5,6].

1.2 The need for a simplified model

A fully detailed cantilever finite element model would require solid elements, contact definitions at joints, friction coefficients and clearance gaps. Such detail may be useful for local stress checks or joint failure investigation. However, it becomes impractical when the cantilever has to be included in a fully constructed OHL model. Pantograph-catenary simulation is already computationally demanding. Gregori et al. [7] addressed this type of cost problem using a two-stage FE method. OSCAR [8], PantoCat [9], PrOSA [10] and PACDIN [11] also use system-level representations of the wire-pantograph interaction, combining finite element, multibody, contact and simplified modelling approaches rather than local solid models of every bracket and joint.

The same modelling constraint applies to the cantilever. If cantilever flexibility is to be used in future pantograph-catenary co-simulation, the cantilever cannot be inserted as a full solid assembly. A simplified structural model is needed, but it must still preserve the stiffness and displacement behaviour during dynamic testing. The use of beam elements is consistent with previous overhead-line modelling work. In most traditional literature, finite element methods have been used to represent catenary behaviour, rigid overhead system components and railway cantilever structures [12,13,14]. These references support the finite element route used here. In this study, the physical members are represented by beam elements with equivalent section properties. The connections are represented using rigid, pinned or restricted connector conditions. This keeps the model focused on global displacement and stiffness, rather than local contact stress or bearing-stress analysis

The simplified model still requires validation. A beam model can reproduce the global cantilever geometry and overall structural response. However, the connection behaviour in the real assembly may differ from the joint conditions used in the model. Joint clearance, friction, local flexibility and seating can change both stiffness and displacement. The model cannot be accepted on geometry and element choice alone. It must be checked against the measured behaviour of the physical cantilever. This comparison measures the error introduced by the simplified model. The model is assessed through global displacement and stiffness, not through local bolt, pin or contact stress.

1.3 Significance of stiffness extraction

Stiffness extraction is required because a simplified cantilever model must represent real mechanical behaviour, not just the external shape of the structure. If it is represented by a spring or spring-damper term, the stiffness value must be supplied. This value cannot be selected randomly without introducing error in the modelling. Support flexibility or stiffness affects contact wire uplift, force transfer and pantograph contact-force variation during motion. This has already been shown in pantograph-catenary research. López-García et al. [15] showed that stiffness and contact modelling influence the predicted dynamic interaction between the pantograph and catenary. Hu et al. [16] later measured equivalent support stiffness in overhead conductor rail systems and used those measured values to improve current-collection simulation models. These studies show that stiffness is not only a structural result rather an input parameter for predicting current-collection behaviour.

The simplified model also assumes that one stiffness value can represent a given cantilever type, direction and configuration. That assumption is only valid if the measured force-displacement response is repeatable and close to linear. Real joints can break this assumption. Song et al. [17] showed that jointed beam structures can develop micro-slip at interfaces, changing stiffness and damping behaviour. Claeys et al. [18] experimentally showed that friction joints produce hysteresis loops and energy dissipation during cyclic loading. Li et al. [19] showed that bolted joint beams can develop nonlinear response because of frictional contact at the joint interface . The tests in this paper connect the simplified model and stiffness problem. They check whether the beam model predicts the measured displacement with acceptable accuracy. They also check whether the measured response can be represented by one stiffness value or needs a nonlinear stiffness description.

2 Methods

2.1 Cantilever configurations and load definition

Two cantilever types were investigated. These were SIC and Bonomi cantilevers. Each was tested in push-off and pull-off configurations. The Bonomi cantilever, pictured in Figure 2, is a triangulated bracket system consisting of a main beam and an inclined triangulating strut. The latter is a pin-adjustable telescopic structure consisting of an outer hollow rectangular tube and an inner sliding member with positional adjustment provided by a pin. Both main beam and triangulating strut are connected to the mast through double-hinged articulation that allows both vertical-plane and lateral-plane rotation. The SIC cantilever, pictured in Figure 3, has a more traditional cantilever design. It consists of a main frame, insulator, main circular beam and registration arm. It is connected to the mast using a hinge.

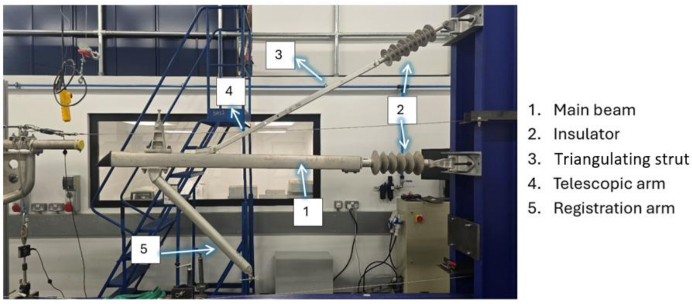

Figure 2: Bonomi cantilever.

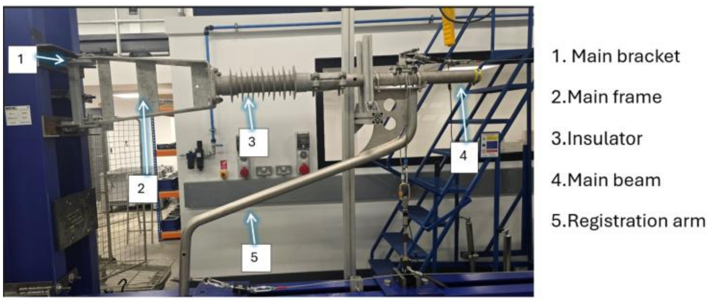

Figure 3: SIC cantilever.

The load case used in this paper for both FEA analysis and quasi-static testing is stated in Table 1. It represents the highest threshold load for serviceability condition according to BS EN 50119, NR/L2/CIV/073 and NR/L2/CIV/072 and UK Master Series internal documents [4,5,6]. The vertical action comes mainly from wire self-weight and ice. The horizontal actions come from wind, stagger and wire tension effects around bends. The contact-wire horizontal action was applied at the registration-arm end as an equivalent force. This represents the structural point where the steady arm transfers the contact-wire load into the cantilever assembly. The steady arm itself was not included in the model or test setup because it acts primarily as a tension member between the contact wire and the registration arm. This avoids modelling a secondary component while still applying the contact-wire action at the correct structural interface.

Force component	Symbol	Magnitude [N]	Direction	Application point
Horizontal force on messenger wire	F_{Mh}	827.69	horizontal	messenger wire attachment
Horizontal force on contact wire	F_{Ch}	938.28	horizontal	registration-arm end
Vertical force on messenger wire	F_{Mv}	1444.00	vertical downward	messenger wire attachment

Table 1: Load Case A force components.

2.2 Simplified finite element model

The finite element models were developed in Abaqus using B31 Timoshenko beam elements. This element type retains axial, bending, shear and torsional behaviour while avoiding the mesh size and contact-convergence problems of a detailed solid assembly. Each physical member was represented by its centreline and equivalent section properties. The mast attachment was fully fixed, and the three loads mentioned in Table 1were applied as concentrated forces at the corresponding wire attachment nodes.

The SIC assembly was treated as a beam-like structure with rigid bolted connections which is reasonable compared to real life structure. This is reasonable because the SIC has fewer clearance-sensitive joints than the Bonomi assembly. The Bonomi assembly was represented by expressing the main beam and triangulating strut as beam elements. The telescopic pin joint in the triangulating strut was replaced with a 1-D translator joint with restricted tolerance. The hinge joints on the mast side were excluded and replaced with a fixed boundary condition. These joint simplifications are more severe because the real Bonomi assembly contains clevises, pins and joint clearances that can add extra movement at the connections. The model was deliberately limited in scope. It was intended to predict global displacement and provide a support representation that could later be transferred into a pantograph-catenary model. It was not intended to predict local contact pressure, bolt slip or pin-bearing stress.

2.3 Experimental quasi-static testing

A custom quasi-static rig applied the three loads from Table 1 to the physical cantilevers. The cantilever was mounted to a steel loading frame in a representative orientation. Loads were measured using calibrated load cells, and displacements were measured at the contact and messenger wire attachment regions using single-axis draw wire displacement sensors. The rig is illustrated in Figure 4. Data acquisition was carried out using a Speedgoat unit running a Simulink model.

Each configuration was tested over five loading cycles. In each cycle, the load was increased quasi-statically from zero to the target value and then returned to zero. Cycling was used because jointed structures often show seating, clearance take-up or slip during early cycles. Repeating the test made it possible to separate stable response from individual mechanical events, instead of treating all cycles as identical.

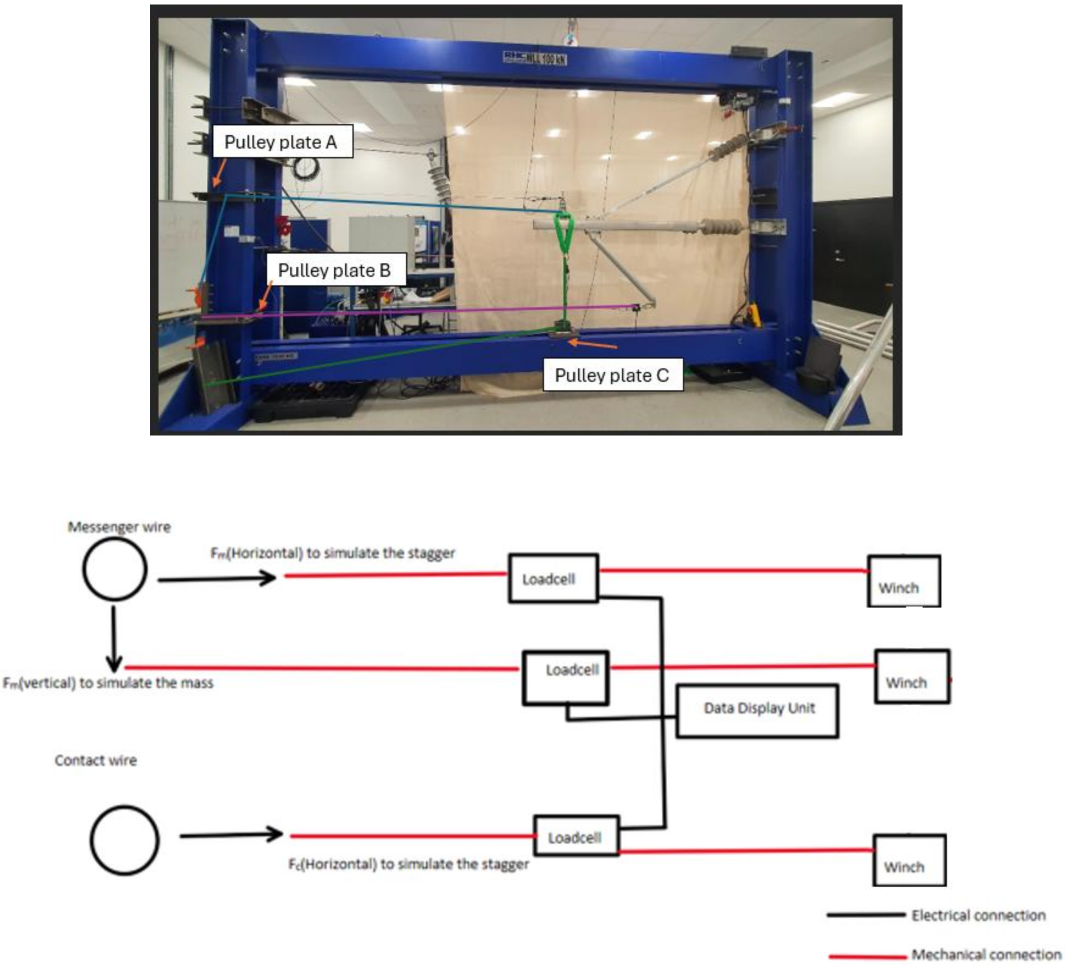

Figure 4: Cantilever testing rig.

2.4 Data processing and behaviour assessment

The cyclic displacement records showed a residual displacement after unloading. This occurred because the loading and unloading cycle data did not coincide. Before each cycle was assessed, the starting displacement was subtracted from all points in that cycle. This gave each cycle the same zero-displacement reference. The correction did not change the force-displacement curves. The hysteresis loop was retained. Only the starting offset from the previous cycle was removed. Then, maximum displacement was extracted for each cycle and summarised using the mean, standard deviation and coefficient of variation. This was used to check repeatability and identify cycles affected by seating or slip. Stiffness was then extracted from the slope of the relevant force-displacement curve. A single linear stiffness was considered suitable only where the loading and unloading behaviour was consistent and repeatable. Otherwise, a nonlinear or bilinear representation was treated as more appropriate.

3 Results

There was no noticeable displacement when load was applied to simulate the horizontal load on the messenger wire. Thus, it has been omitted due to insignificance. So, in this paper, horizontal load or displacement refer to the result of simulated F_{Ch} and vertical load or displacement refers to the result of simulated F_{Mv}.

3.1 Finite element baseline

Table 2 gives the Abaqus predictions under Load Case A. The SIC model is much more flexible than the Bonomi model according to the finite element results. In horizontal displacement, the Bonomi push-off prediction is only 2.80 mm compared with 22.15 mm for SIC push-off. In pull-off, the Bonomi prediction is 0.83 mm compared with 10.50 mm for SIC. This difference is mainly caused by the simplified connection assumptions in the Bonomi model. Samples of the deformed Bonomi and SIC cantilever models are presented in Figure 5.

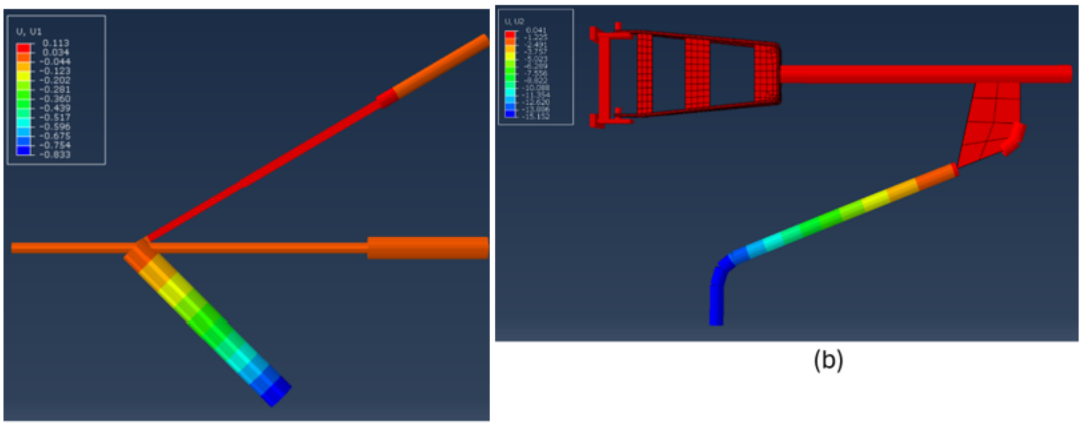

(b)

(a)

Figure 5: Deformed model after load application. (a) Bonomi pull off mode horizontal displacement (mm); (b) SIC pull off mode vertical displacement (mm).

Configuration	Contact wire horizontal [mm]	Messenger wire vertical [mm]
SIC push-off	22.15	7.23
SIC pull-off	10.50	0.60
Bonomi push-off	2.80	0.54
Bonomi pull-off	0.83	0.25

Table 2: FE prediction of displacement for cantilever under operational load.

3.2 Experimental repeatability and cycle selection

Table 3 summarises the processed experimental displacement values. The mean displacement for the SIC displacement uses Cycles 1 to 5 in all cases. The Bonomi push-off vertical displacement excludes Cycle 1 because it represents initial seating.

Bonomi pull-off uses Cycles 2, 3 and 5 because Cycle 1 shows seating and Cycle 4 shows a joint-movement anomaly.

Configuration	Direction	Cycles used	Mean disp. [mm]	SD [mm]	CoV [%]
SIC push-off	contact horizontal	1-5	18.12	1.01	5.6
SIC push-off	messenger vertical	1-5	20.40	1.06	5.2
SIC pull-off	contact horizontal	1-5	10.58	0.74	7.0
SIC pull-off	messenger vertical	1-5	1.54	0.15	9.8
Bonomi push-off	contact horizontal	1-5	10.24	0.22	2.1
Bonomi push-off	messenger vertical	2-5	2.12	0.17	8.0
Bonomi pull-off	contact horizontal	2, 3 and 5	5.53	0.21	3.8
Bonomi pull-off	messenger vertical	2, 3 and 5	1.67	0.06	3.5

Table 3: Experimental maximum displacement summary and repeatability statistics.

3.3 Validation of the simplified beam model compared to FEA model

Table 4 and Figure 6 show the comparison between the FEA and experimental data. The ratio of FEA to experimental mean data shows the direction of the modelling bias. A value close to 1 means the displacement level is captured by FEA accurately. A value below 1 means the finite element model is too stiff and vice versa.

The strongest validation result is for SIC (pull-off) horizontal response. The FEA prediction is 10.50 mm and the experimental mean average is 10.58 mm. This gives a ratio of 0.99 and an error of 0.8 percent. SIC push-off horizontal response is less exact but still comparable (ratio 1.22). These results show that the beam model captures the SIC horizontal response reasonably well. In this direction, bending of the registration arm dominates the response.

The SIC vertical response does not match the FEA as closely. In push-off, the FEA predicts 7.23 mm, compared with 20.40 mm in the test. In pull-off, it predicts 0.60 mm, compared with 1.54 mm in the test. These differences are due to modelling the SIC mast connection as being rigid. Hence, the FEA model only simulates bending of the main beam, insulator and main frame, due to the moments applied by the vertical messenger wire load and the off-axis, horizontal contact wire load. In the real system, compliance within the main bracket hinge system, under moment loading, allows a significant amount of rigid body rotation of the cantilever, resulting in vertical displacement at the messenger wire support point. This is more pronounced in the push off mode as the moments due to the two forces are in the same direction.

The Bonomi results show a different type of discrepancy. In push-off, the horizontal FEA prediction is only 27 percent of the experimental displacement. In pull-off, it is only 25 percent. The same pattern appears vertically. This is not a random test problem because the CoV values are low when considering stable cycles. It is a repeatable modelling error caused by connection flexibility that is not present in the simplified Bonomi FEA model.

Configuration	Direction	FEA [mm]	Experimental mean [mm]	FEA/ Exp	Error %	Reading
SIC push-off	contact horizontal	22.15	18.12	1.22	22.2	same order, moderate error
SIC push-off	messenger vertical	7.23	20.40	0.35	64.6	vertical mismatch
SIC pull-off	contact horizontal	10.50	10.58	0.99	0.8	strong match
SIC pull-off	messenger vertical	0.60	1.54	0.39	61.0	vertical mismatch
Bonomi push-off	contact horizontal	2.80	10.24	0.27	72.7	FEA too stiff
Bonomi push-off	messenger vertical	0.54	2.12	0.25	74.6	FEA too stiff
Bonomi pull-off	contact horizontal	0.83	5.53	0.15	85.0	FEA too stiff
Bonomi pull-off	messenger vertical	0.25	1.67	0.15	85.0	FEA too stiff

Table 4: Finite element validation against processed experimental displacement.

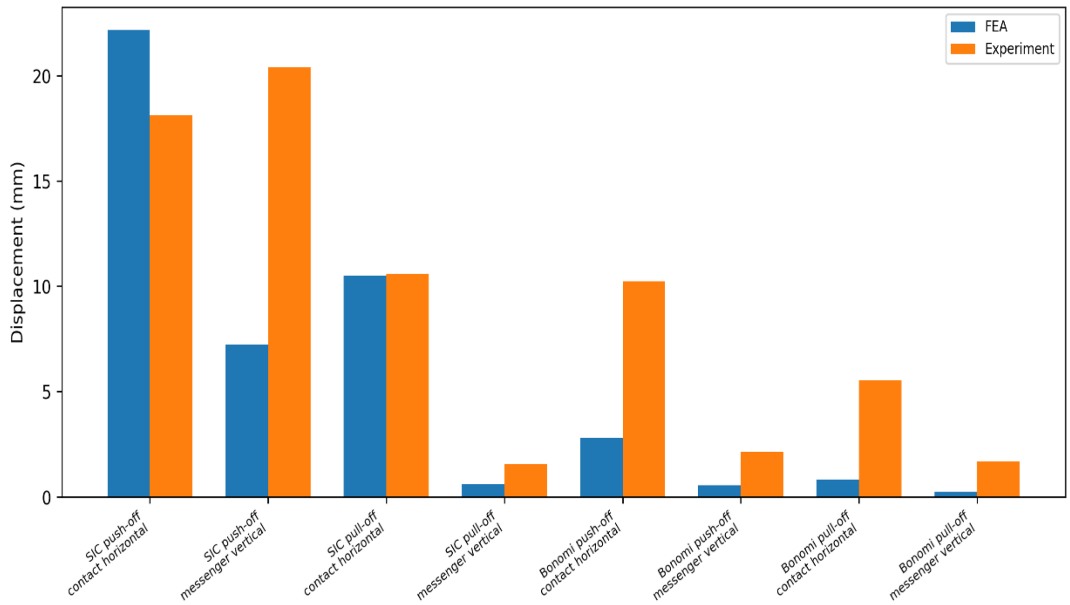

Figure 6: Finite element predictions compared with processed experimental mean displacements.

3.4 Stiffness extraction

Table 5 reports the stiffness measured during the loading and unloading, while Figure 7 shows the same comparison graphically. The loading vs. unloading percentage difference is included to show whether the response can be treated as one spring-like value or whether the loading history matters. Large percentage difference indicates a single stiffness value would fail to accurately capture the actual behaviour of the cantilever. Table 5 shows the effect of configuration on stiffness. SIC messenger vertical stiffness increases from 49.90 N/mm in push-off to 900.9 N/mm in pull-off, which is about 18 times higher for the same cantilever. The loading and unloading cycles also affect stiffness. For Bonomi pull-off, its horizontal stiffness drops from 172.4 N/mm during loading to 86.96 N/mm during unloading. It is a difference of about 50 percent. Interestingly, its vertical unloading stiffness also changes with force range. The unloading stiffness is 357.1 N/mm above 400 N and 2000 N/mm below 400 N. These values show why the stiffness table is not just a list of slopes. It identifies which cases are suitable for one effective spring value and which ones need a more detailed stiffness description.

Configuration	Direction	Loading [N/mm]	Unloading [N/mm]	Loading vs unloading [%]
SIC push-off	contact horizontal	68.35	68.35	0.0
SIC push-off	messenger vertical	49.90	49.90	0.0
SIC pull-off	contact horizontal	97.09	89.29	8.0
SIC pull-off	messenger vertical	900.9	826.5	8.3
Bonomi push-off	contact horizontal	87.72	86.96	0.9
Bonomi push-off	messenger vertical	666.7	666.7	0.0
Bonomi pull-off	contact horizontal	172.4	86.96	49.6
Bonomi pull-off	messenger vertical	769.2	Load dependent; 357.1 N/mm above 400 N; 2000 N/mm below 400 N	force dependent

Table 5: Extracted stiffness values and recommended simplified representation.

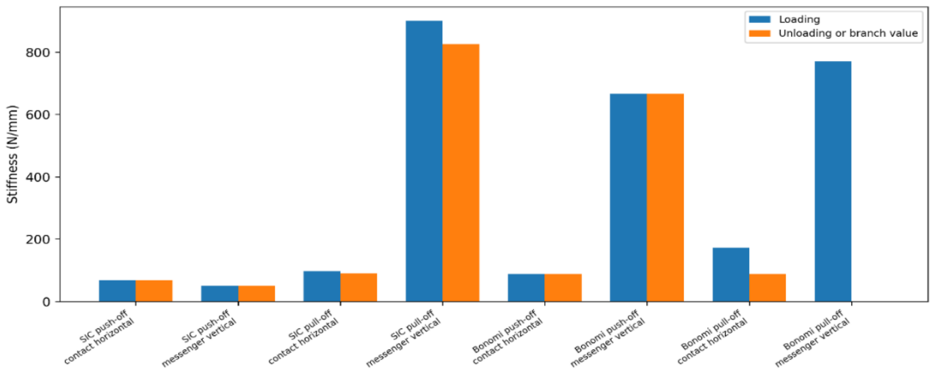

Figure 7: Loading and unloading stiffness values.

Figure 8 gives representative curves for a repeatable case and a joint-controlled case. SIC push-off in Figure 8(a) is almost linear and repeatable. Bonomi pull-off in Figure 8(b) is less consistent. Pin and clevis movement causes seating, branch changes and force-range effects. These appear as nonlinear force-displacement behaviour.

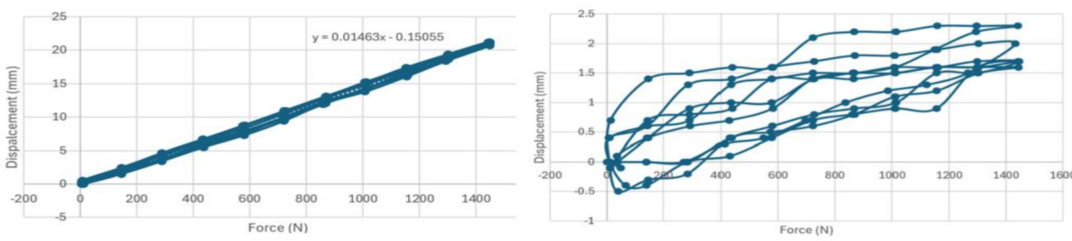

(a) (b)

Figure 8: Representative cyclic responses showing a repeatable case and a joint-dominated case. Showing 5 load cycles for messenger wire vertical displacement (a) SIC push-off (b) Bonomi pull off mode.

This interpretation is consistent with the joint literature. Song et al. [17] showed that jointed beams can develop micro-slip at interfaces. Claeys et al. [18] showed that friction joints produce hysteresis and energy dissipation during cyclic loading. Li et al. [19] showed that bolted joint beams can become nonlinear due to frictional contact.

3.5 Simplified-model analysis

The following points translate the numerical results into modelling choices.

- SIC push-off: The simplified model gives the correct order of horizontal displacement. So, the beam model can be used for horizontal displacement. The vertical stiffness should be taken from the test.
- SIC pull-off: This is the strongest validation case for the simplified model. This configuration should keep the beam model for horizontal response. For stiffness-based modelling, the eight percent branch change suggests that separate loading and unloading stiffness values are better if hysteresis is being represented.

- Bonomi push-off: The test response is repeatable, but the simplified model is too stiff. The horizontal prediction is 2.80 mm against 10.24 mm in the test. The vertical prediction is 0.54 mm against 2.13 mm after the seating cycle is removed. This points to pin, clevis and seating movement that is not represented in the current model. The beam geometry should be kept, but the joints should be corrected with an experimentally validated effective spring or connector stiffness.
- Bonomi pull-off: This configuration needs the most correction. The model predicts only about 15 percent of the measured displacement in both measured directions. The horizontal stiffness changes from 172.4 N/mm during loading to 86.96 N/mm during unloading. The messenger-vertical unloading response also changes around 400 N. This case should not use one constant stiffness. It should use separate loading and unloading stiffness values or a bilinear connector law at the relevant hinge locations.

Overall, the simplified beam model should be retained as the primary geometry. It works best where displacement error is low and stiffness behaviour is stable. Where the response is repeatable but the FEA error is high, the model needs calibrated stiffness added to the joints. This is the practical route for Bonomi. The next model should keep the beam members and replace rigid or pinned connection assumptions with calibrated hinge or connector behaviour. Those connector values can be identified from the quasi-static force-displacement data and future tests.

3.6 Model error and interpretation limits

The error check separates model error from experimental repeatability. SIC pull-off (for F_{Ch}) mode is the strongest case. The FEA error is 0.8 percent and the experimental CoV is 7.0 percent. In this case, the model error is smaller than the cycle variation. Bonomi is different. Bonomi push-off (for F_{Ch}) has 72.7 percent FEA error against 2.1 percent CoV. Bonomi pull-off (for F_{Ch}) has 85.0 percent error against 3.8 percent CoV. These errors are far beyond the repeatability range. They point to missing connection flexibility rather than unstable measurements.

Two limits should be kept in mind. First, the simplified models do not include the full behavior of the connections. This has the largest effect on the Bonomi cantilever because it contains pins, clevises and joint movement. Second, the displacement sensors measure one direction, while the cantilever can translate and rotate under combined loading. This matters most in the vertical comparisons because the predicted vertical movements are small. These limits do not remove the main conclusion. They explain why the simplified model needs experimental stiffness correction before it is used in future pantograph-catenary modelling.

4 Conclusions and Contributions

This paper developed and tested simplified beam-element finite element models of Bonomi and SIC cantilevers under operational quasi-static loading. The simplification is necessary because full solid-contact modelling of bolts, pins, friction and clearances is not practical for repeated pantograph-catenary simulation.

The simplified model represented the SIC horizontal response most successfully. The SIC pull-off horizontal case gave the closest agreement, while SIC push-off horizontal response showed moderate error. This supports the beam-element approach where the response is governed mainly by member bending and stiff bolted connections. The Bonomi response was not captured with the same accuracy because pin clearance, seating and small connection movement are more sensitive in Bonomi. Those errors define the limit of the simplification rather than invalidating it.

The measured stiffness values ranged from 49.90 N/mm to 900.9 N/mm, giving an eighteenfold configuration-dependent variation. This shows that one generic cantilever stiffness is not adequate for the tested configurations. Push-off cases were more suitable for a linear spring representation. Pull-off cases required nonlinear or bilinear treatment due to joint movement during loading and unloading.

The main contribution is a practical route for reducing real cantilever hardware into usable co-simulation parameters. Maximum displacement comparison quantifies the error of the beam idealisation, while stiffness extraction supplies the spring values needed for future dynamic characterisation. Future work should use multi-axis displacement measurement, hammer or shaker testing, and calibrated connector models so that stiffness, effective mass and damping can be integrated into pantograph-catenary co-simulation.

Acknowledgements

The authors would like to thank University of Huddersfield for use of their Civil Engineering Laboratory.

References

[1] Lesics, "The fascinating engineering behind electric trains!", YouTube video, 2022, https://www.youtube.com/watch?v=GJbUI2D3rLY.

[2] G. Keenor, P. Hooper, P. Dearman, "An introduction to the overhead electric traction system", The PWI Journal, 139(2), 24-31, 2021,

[3] A. Milne, "Alstom - the CLever Innovator", Rail Engineer, 2017, https://www.railengineer.co.uk/alstom-the-clever-innovator/.

[4] British Standards Institution, "BS EN 50119:2020 Railway applications. Fixed installations. Electric traction overhead contact lines", BSI, London, United Kingdom, 2020, DOI:10.3403/30341014U.

[5] Network Rail, "NR/L2/CIV/073 Design of Overhead Line Structures", Network Rail, London, United Kingdom, 2015.

[6] Network Rail, "NR/L2/CIV/072 Wind Loading of Overhead Line Equipment and Structures", Network Rail, London, United Kingdom, 2019.

[7] S. Gregori, M. Tur, E. Nadal, J.V. Aguado, F.J. Fuenmayor, F. Chinesta, "Fast simulation of the pantograph-catenary dynamic interaction", Finite Elements in Analysis and Design, 129, 1-13, 2017, DOI:10.1016/j.finel.2017.01.007.

[8] J.-P. Massat, E. Balmes, J.-P. Bianchi, G. Van Kalsbeek, "OSCAR statement of methods", Vehicle System Dynamics, 53(3), 370-379, 2015, DOI:10.1080/00423114.2015.1005016.

[9] J. Ambrosio, J. Pombo, P. Antunes, M. Pereira, "PantoCat statement of method", Vehicle System Dynamics, 53(3), 314-328, 2015, DOI:10.1080/00423114.2014.969283.

[10] L. Finner, G. Poetsch, B. Sarnes, M. Kolbe, "Program for catenary-pantograph analysis, PrOSA statement of methods and validation according EN 50318", Vehicle System Dynamics, 53(3), 305-313, 2015, DOI:10.1080/00423114.2014.958501.

[11] M. Tur, L. Baeza, F.J. Fuenmayor, E. Garcia, "PACDIN statement of methods", Vehicle System Dynamics, 53(3), 402-411, 2015, DOI:10.1080/00423114.2014.963126.

[12] O. Lopez Garcia, A. Carnicero Lopez, J.L. Marono Martinez, "Influence of stiffness and contact modelling on catenary-pantograph system dynamics", Journal of Sound and Vibration, 299(4-5), 806-821, 2007, DOI:10.1016/j.jsv.2006.07.018.

[13] X. Feng, Z. Hu, S. Gao, F. Duan, W. Chu, Y. Song, "Modelling and analysis of expansion joints' effect on dynamic performance of railway rigid overhead system", Sensors, 23(15), 6797, 2023, DOI:10.3390/s23156797.

[14] V. Patil, I. Jain, R. Upasani, G. Bhoye, S. Zanje, "Design and analysis of robust modular cantilevers for railway overhead applications: a failure prevention approach", Journal of Failure Analysis and Prevention, 24, 1148-1165, 2024, DOI:10.1007/s11668-024-01903-z.

[15] Z. Hu, Y. Song, L. Chen, F. Duan, Z. Liu, X. Feng, "Experimental and numerical exploration of support stiffness influence on the current collection quality of pantograph and overhead conductor rail system", IEEE Transactions on Transportation Electrification, 10(3), 7112-7126, 2024, DOI:10.1109/TTE.2023.3345955.

[16] K.-H. Lee, Y.-H. Cho, J. Chung, "Dynamic analysis of a three-dimensional catenary system using the finite element method", Transactions of the Korean Society of Mechanical Engineers A, 33(11), 1306-1313, 2009, DOI:10.3795/KSME-A.2009.33.11.1306.

[17] Y. Song, D.M. McFarland, L.A. Bergman, C.J. Hartwigsen, A.F. Vakakis, "Modeling of the dynamics of jointed beam structures", Proceedings of the ASME Design Engineering Technical Conference, Chicago, United States, 1091-1100, 2003, DOI:10.1115/DETC2003/VIB-48434.

[18] M. Claeys, J.-J. Sinou, J.-P. Lambelin, R. Todeschini, "Experiments and numerical simulations of nonlinear vibration responses of an assembly with friction joints", Mechanical Systems and Signal Processing, 70-71, 1097-1116, 2016, DOI:10.1016/j.ymssp.2015.08.024.

[19] D. Li, C. Xu, D. Wang, "Numerical modeling and analysis of nonlinear dynamic response for a bolted joint beam considering interface frictional contact", Proceedings of the ASME International Mechanical Engineering Congress and Exposition, Pittsburgh, United States, 2018, DOI:10.1115/IMECE2018-86743.